Study of the Processes of Forming a Metal Coating by Cold Gas-Dynamic Sputtering and Development of a Technique for Calculating Sputtering Modes

O. L. Haydamak and V. F. Hraniak

Vinnytsia National Agrarian University,
3 Sonyachna Str.,
UA-21008 Vinnytsia, Ukraine

The creation of various functional coatings on the surfaces of parts allows to influence the technical and operational characteristics of the parts and to give to these parts new qualities extrinsic for parts without coating. The principle of creating coatings is based on the effect discovered in the 1980s of the previous century, which consists in the fact that powder particles accelerated to high speeds close to the speed of sound, when they collide with the substrate, enter into molecular bonds with it and are able to form a strong connection both with the latter and between its own dispersed particles themselves. At the same time, the temperature of the powder coating process is significantly lower than the melting point of the powder coating material. The installation for cold-gas-dynamic spraying of metal coatings is designed and manufactured. The main components of this installation are a compressed air heater and a nozzle-accelerator of heated compressed air. In accordance with the ejection effect, finely dispersed metal powder with an average particle size of $60\,\mu m$ is fed into the nozzle, which accelerates in the nozzle channel and, because of heat exchange with hot air, is heated to a temperature that is significantly lower than the melting point of the powder material. As a result, the part and powder material do not undergo phase transformations and, accordingly, do not change their properties and do not undergo significant thermal deformations. The patterns of sputtering shape formation using powder based on aluminium grade A20-11 are studied. As established, the formation of the sputtering shape profile in the general case can be described in accordance with the Gaussian-distribution law. After ana-

Corresponding author: Oleh Leonidovych Haydamak
E-mail: vntu111@gmail.com

lysing the relative deviation of the Gaussian function from the experimental profile of the sputtering figure, it is established that the largest deviations of the theoretical figure from the experimental one are observed at the periphery of the sputtering figure with a coating thickness not exceeding 0.1 mm; and the smallest deviation occurs in the middle zone on the axis of the sputtering figure, where there is the place of the most intensive formation of the coating. Considering the above, it can be concluded that the Gaussian distribution describes the shape of the sputtering figure profile with great reliability. The average integral relative error of the Gaussian function does not exceed 9%. A methodology for modelling the coating creation process is proposed, which allows predicting the shape of the sprayed figure profile depending on the productivity of the spraying device. This profile enables to establish an optimal interval between adjacent passes of the nozzle-accelerator over the surface of the workpiece. The proposed method allows to calculate the optimal nozzle-accelerator movement speed relative to the workpiece, the rotational speed of the workpiece, the required amount of powder for coating a given workpiece, the spraying time, and reducing unnecessary powder losses to a minimum, considering the productivity of the coating creation process and the powder utilization coefficient.

Key words: gas-dynamic sputtering, sputtering shape, calculation of movement speed.

В основі принципу створення покриттів покладено ефект, який полягає в тому, що порошкові частинки, розігнані до швидкости у понад 360 м/с, за потрапляння на поверхню деталю утворюють з ним зв'язки на молекулярному рівні, що приводить до утворення міцного з'єднання як покриття з деталем, так і між власне дисперсними частинками порошку, який напорошується. В процесі створення покриття температурний режим, потрібний для реалізації процесу нанесення порошкового покриття, є істотно нижчим за температуру топлення матеріялу порошкового покриття. Спроєктовано та виготовлено установку для холодного газодинамічного напорошення металевих покриттів. Основними складовими цієї установки є нагрівач стиснутого повітря та сопло-пришвидшувач нагрітого стиснутого повітря. Встановлено, що формування профілю фіґури напорошення у загальному випадку може бути описано у відповідності до закону Ґауссового розподілу. Аналізою відносного відхилу Ґауссової функції від профілю експериментальної фіґури напорошення встановлено, що найбільші відхили останньої спостерігаються на периферії фіґури напорошення з товщиною покриття, що не перевищує 0,1 мм, а найменші відхили спостерігаються в середній зоні на осі фіґури напорошення, в якій має місце найбільш інтенсивне формування покриття. Враховуючи сказане, можна дійти висновку, що розподіл порошкових частинок за формування фіґури напорошення у відповідності до Ґауссової функції з достатньо великою правдоподібністю описує процес формування фіґури газодинамічного напорошення, похибка якої є незначною і не перевищує 9%. Запропоновано методику моделювання процесу створення покриття, яка дає змогу прогнозувати форму профілю фіґури напорошення в залежності від продуктивности напорошувального пристрою. Методика уможливлює в залежності від продуктивности процесу створення покриття та коефіціє-

нта використання порошку розрахувати оптимальну швидкість переміщення сопла-пришвидшувача відносно деталю, швидкість обертання деталю, необхідну кількість порошку для покриття заданого деталю, час напорошення та звести до мінімуму нераціональні втрати порошку.

1. INTRODUCTION

Creation of various functional coatings on surfaces of component parts allows influencing their technical and operational characteristics and confers to them new qualities that are not inherent in component parts without a coating. For example, application of copper- or aluminium-based coatings on the surfaces of steel component parts can protect such surfaces against corrosion and significantly change frictional and conductive properties of coated surfaces.

At the Department of Power Engineering, Electrical Engineering and Electromechanics of Vinnytsia National Agrarian University, an experimental unit for gas-dynamic application of functional coatings was developed and manufactured. The principle of operation of the experimental unit is based on the discovery made in the 1980's of the previous century [1, 2], which consists in the fact that powder particles are accelerated to high velocities close to the sound speed and heated to temperatures significantly lower than their melting temperature, upon contact with the surface, the component parts enter into molecular bonds with it, being able to form a strong connection both with the latter and between adjacent dispersed particles of sprayed powder. At the same time, powder particles' heating temperature is much lower than their melting temperature.

Development of gas-dynamic sputtering technology is becoming increasingly widespread due to the ease of coating formation, the absence of harmful environmental effects, an insignificant thermal effect on the sputtering object, the absence of phase transformations of the material of the component part being coated and the coating itself, the absence of oxidation processes on surfaces of the component part and the coating, the opportunity to change the tribological characteristics of surface layers of the component part, generation of electrically conductive and electrically insulating coatings, and anticorrosion protection of surfaces [3–14].

The purpose of the research paper is the experimental study of sputtered solid and component part surface formation, as well as development of the techniques for calculation of cold-gas-dynamic sputtering modes based on experimental results.

2. RESEARCH OBJECT AND METHODS

Functional coatings were created on the experimental cold gas-dynamic sputtering unit designed and manufactured at the Department of Power Engineering, Electrical Engineering and Electromechanics of Vinnytsia National Agrarian University (Fig. 1).

The unit is connected to the compressor that supplies compressed air to heater *1*, which consists of ceramic channels, in the middle of which the heating element (nichrome spiral) is located. Passing around the full-hot spiral, compressed air is heated because of heat exchange to a certain temperature (300–400°C), which is controlled by the thermocouple built into the heated compressed air accelerator nozzle.

The heated compressed air accelerator nozzle (Fig. 2) consists of housing *1* containing the sputtering channel, compressed air supply channel *2* and channel *3*, through which the sputtering powder is supplied. From the heater through channel *2*, heated compressed air enters the accelerator nozzle, where it passes through the annular gap between cone *4* and channel *1*. Due to cone *4* in the housing channel, the air flow is accelerated and its pressure drops below the atmospheric one, which causes the ejection effect and leads to the sputtering powders' suction through channel *3* and its mixing with the flow of heated compressed air.

Because of heat exchange, the powder is heated and accelerated in the nozzle to supersonic speed depending on the pressure of the compressed air. When powder particles hit the surface of the component part, to which the coating is applied, the powders' molecular bonds
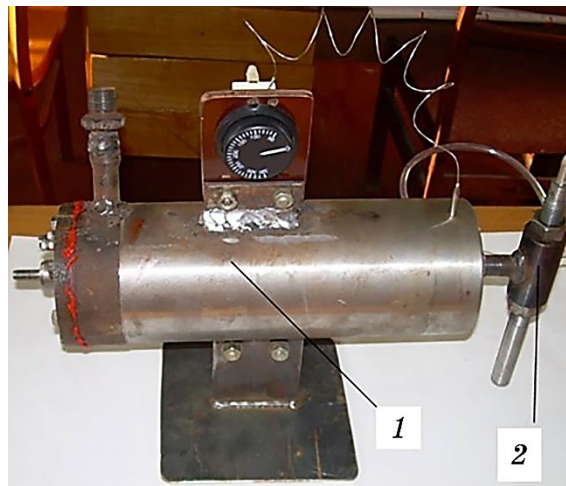

Fig. 1. Experimental unit for gas-dynamic application of functional coatings: compressed air heater (*1*), heated compressed air accelerator nozzle (*2*).
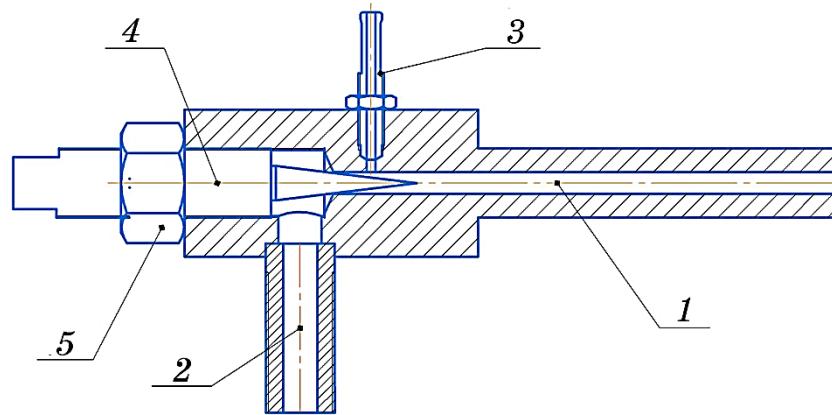
Fig. 2. Nozzle. Housing with the sputtering channel (*1*), compressed air supply channel (*2*), sputtered powder material supply channel (*3*), cone (*4*), lock nut (*5*).

arise both with the material of the component part and between neighbouring powder particles, which leads to formation of a continuous coating. The nozzle design allows adjusting the parameters of the gas-powder flow by moving cone *4* relative to cone *1*, as a result of which the annular gap between them changes, this, accordingly, leading to a change in the velocity and pressure of the gas-powder flow. Specific features of the design of such a nozzle are detailed in [13].

A20-11 brand powder was used for sputtering. During the experiment, three portions of powder of different weights were formed: the first one—0.11 g, the second one—0.22 g and the third one—0.34 g. The sputtering distance was 25 mm, the temperature of the compressed air was 320–340°C. Compressed air pressure was of 0.56 MPa.

As a result of the experimental study, three sputtered solids were obtained, the photos of which are shown in Fig. 3.
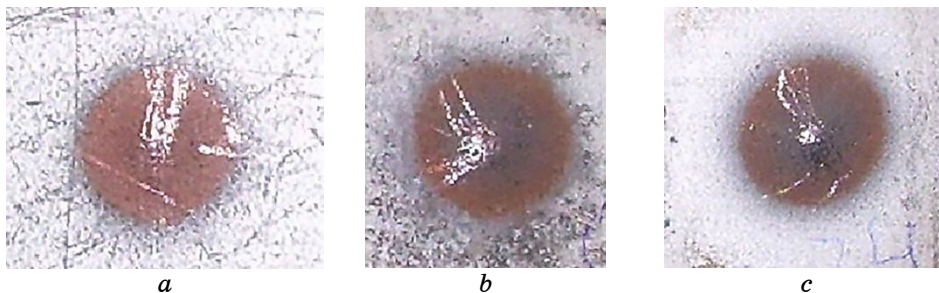

Fig. 3. Sputtered solids the first one—0.11 g (*a*), the second one—0.22 g (*b*), the third one—0.34 g (*c*).

Fig. 4. Measurement of the sputtered solid profile shape.

With the use of a watch-type micrometer and PMT-3 microhardness meter table **(Fig. 4)**, the height of each solid profile was measured in 0.25 mm steps.

3. EXPERIMENT RESULTS AND DISCUSSION THEREOF

Based on the results of the measurements, the profiles of all sputtered solids were constructed, which are shown by dotted lines in Fig. 5.

In the cross-section, obtained sputtered solids are almost symmetrical relative to their axes, and their profile can generally be described in accordance with the Gaussian distribution law. To describe the shape of the cross-section of the sputtered solids, the Gaussian curve was assumed as follows:

$$Y = y_0 e^{-r^2/r_0^2} , \tag{1}$$

where y_0 is the coating thickness on the sputtered solid axis, Y is the height of the profile depending on the distance from the solid r, r_0 axis—scattering radius (chosen empirically to ensure the best match between the Gaussian curve and experimental results). $y_0 = 0.152, 0,41, 0.54$; $r_0 = 1.6, 1.7, 1.55$ for the first and, respectively, the second samples.

Sputtered solid profiles were constructed for sputtered solids according to the Gaussian distribution are shown in Fig. 4 by continuous lines.

Having analysed the relative deviation of the Gaussian function from the experimental profile of the sputtered solid, one can see that the theoretical solid largest deviations from the experimental one is observed on the periphery of the sputtered solid with a coating thickness not exceeding 0.1 mm, and the smallest deviation can be seen in
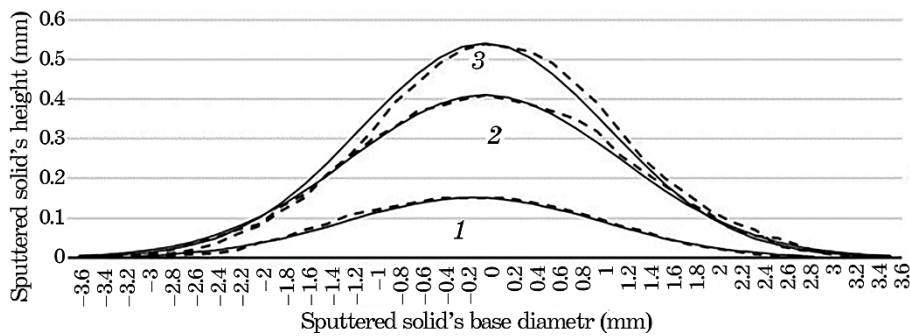
Fig. 5. Comparison of sputtered solid profiles with Gaussian distribution.

the middle zone of the sputtered solid axis, in which the sputtered solid most intensive formation occurs.

Let us compare the obtained Gaussian distributions with the experimental results, for which we impose the theoretical distribution on respective scale on the experimental results (Fig. 5).

Analysing the experimental data, one can note that the Gaussian distribution describes the shape of the sputtered solid profile with a great reliability. The average integral relative error of the Gaussian function does not exceed 9%.

It is worth noting that important factors influencing the powder coating-sputtering mode are the patterns of powder particles' distribution in the airflow during the collision between powder particles with the component part surface. This significantly affects the intensity of the coating build-up. Thus, it can be seen that the intensity of the coating build-up has an uneven character and significantly depends on the distance to the axis of the air–powder flow of the sputtering device. From what has been written follows the technical possibility of forecasting the shape of the sputtered solid and adjusting (changing) the mode of coating creation, which will reduce allowances for further processing and losses of powder material at the stage of designing the technological process of creating the functional coatings by cold-gas-dynamic sputtering.

The main factor that affects the sputtered solid shape is the performance of the coating build-up for different areas of the sputtered solid. Let us determine the coefficient of performance of sputtering particles' flow K_i for each unit cell. This coefficient will determine the coating performance depending on location of the unit cell, *i.e.*, from radius r_i to the sputtering axis, on which the unit cell is located.

$$K_i = Y/H \, , \tag{2}$$

where Y is the Gaussian function (1), H is the height of the sputtered

solid in the case of a uniform coating formation over the entire area of the sputtered solid (with no regard to the Gaussian distribution).

The weight of the sputtered solid m can be determined from the sputtering unit performance P_y (for example, the unit performance $P_y = 0.1$ g/sec)

$$m = P_y t = V\rho = SH\rho,\qquad(3)$$

from which, height H is as follows:

$$H = \frac{P_y t}{S\rho},\qquad(4)$$

y_0 is the sputtered solid height taking into account the Gaussian distribution, ρ—the material sputtered solid density, S—the area of the sputtered solid base, t—the sputtering time.

To determine the sought height, let us analyse the ratio of heights between sputtered solids of the same volume, taking into account the Gaussian distribution and without the same, and namely, when the sputtered solid is formed uniformly as a cylinder. To do this, let us build a 3D model of the sputtered solid in accordance with the Gaussian distribution using Kompas software (Fig. 6) and, using 'Mass-centring characteristics' function, determine this solid volume as in Fig. 7. which, for example, for the sputtered solid shown in Fig. 5, is $V = 5.7138$ mm³.

The comparison of sputtered solids with the same volume taking into account the Gaussian distribution, which has of y_0 height, and the imaginary uniform generation of coating with no regard to the Gaussian distribution is shown in Fig. 8.

Knowing the volume and diameter D_0 of the sputtered solid base, it is not difficult to determine the height of the cylindrical sputtered solid with no regard to the Gaussian distribution:

$$H = \frac{V}{S} = \frac{V}{\pi D_0^2} = \frac{5.7138}{3.1415 \times 7.25^2} = 0.25\,\text{mm}.\,.\qquad(5)$$

Hence, the coefficient of performance of sputtering particles' flow K_i will be as follows:

$$K_i = \frac{y_0}{H} e^{-r_i^2/r_0^2}.\qquad(6)$$

Fig. 6. 3D model of the sputtered solid.

```
 ☼ Информация                                          ×
 ▣ 🖶
 документ
 ----------------------------------------------
 МЦХ модели

 Деталь
 Заданные параметры
 Материал тел            АД0   ГОСТ 4784-97
 Плотность материала тел          Ro =0.002710 г/мм3

 Расчетные параметры(тела и компоненты)
 Масса                           M = 0.015484 г
 Площадь                         S = 83.274250 мм2
 Объем                           V = 5.713787 мм3
 Центр масс                      Xc = -3.267449 мм
                                 Yc = 0.000000 мм
                                 Zc = 0.236256 мм
```

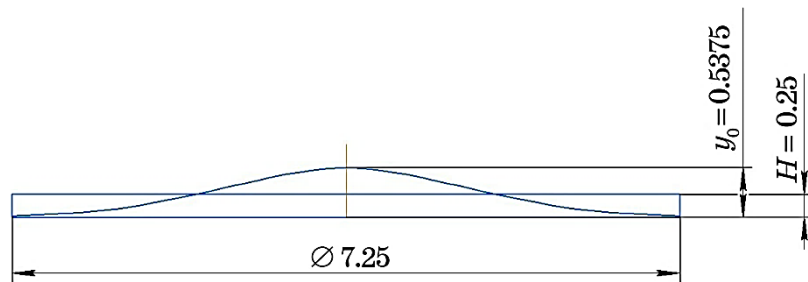**Fig. 7.** Mass-centring characteristics of the sputtered solid.

Fig. 8. Comparison of sputtered solids with the same volume taking into account the Gaussian distribution with y_0 height and in the case of an imaginary uniform coating creation with no regard to the Gaussian distribution, having H height.

Let us find out how the performance will change for each elementary cell taking into account the Gaussian distribution.

The performance of sputtering particles' flow into each elementary cell p_i is as follows:

$$p_i = PK_i = \frac{P_y K_i}{S} = \frac{P_y \dfrac{y_0}{H} e^{-r_i^2/r_0^2}}{S} = \frac{P_y \dfrac{y_0}{P_y t} \rho S e^{-r_i^2/r_0^2}}{S} = \frac{y_0}{t} \rho e^{-r_i^2/r_0^2} , \qquad (7)$$

where $P = P_y/S$ is the average of the sputtering device performance for each unit cell (with no regard to the Gaussian distribution).

Knowing the sputtering device performance and the sputtering time, it is possible to determine the sputtering powder weight for each elementary cell:

$$m_i = p_i t . \qquad (8)$$

Let us find out which profile the sputtered solid will have. To do this, we determine height hi of each cell based on the condition of the elementary cell weight, which is as follows:

$$m_i = s_i h_i \rho . \tag{9}$$

For example, A20-11 powder has the density $\rho = 0.0053 \, \text{g/mm}^3$. From (9), we determine the height of each elementary cell:

$$h_i = \frac{m_i}{s_i \rho} . \tag{10}$$

Into (10), we substitute m_i from (8) and obtain:

$$h_i = \frac{p_i t}{s_i \rho} . \tag{11}$$

The area of the unit cell is selected upon the condition of the sputtering particles' average size in accordance with their diameter d (for example, for aluminium A20-11-based powder, the powder particles' diameter d does not exceed 0.060 mm). Accordingly, the elementary cell area will be as follows:

$$s_i = \frac{\pi d^2}{4} = \frac{3.1415 \times 0.06^2}{4} = 0.00282735 \, \text{mm}^2 . \tag{12}$$

Using the given algorithm, it is possible to simulate the calculated sputtered solids for the given performance of the sputtering device.

4. TECHNIQUES FOR CALCULATION OF TECHNOLOGICAL MODES OF COLD-GAS-DYNAMIC SPUTTERING

The cross-section of simulated sputtered solids can be used to determine the sputtering step between adjacent runs to ensure the most uniform functional coating layer that saves powder materials and reduces post-coating mechanical processing costs.

Let us consider what the most optimal distances (steps) should be between adjacent runs, wherefore we will analyse the designed sputtered solids with different heights and diameters of these solids' bases. (Figs. 9, 10 and 11).

The most uniform coverage can be ensured by providing the distance between adjacent runs, which means the equality of areas of overlap plots *1* and *2*, which are shown in Figs. 9, 10 and 11. This distance is for sputtered solid 1 is 3.2 mm, for 2—3.9 mm, for 3—3.5 mm, which, relative to the diameter of the sputtered solid base, for solid 1 is of 56%, for 2—56%, for 3—48%, respectively, that is, with the increase
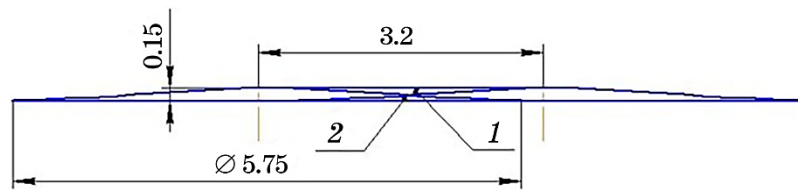
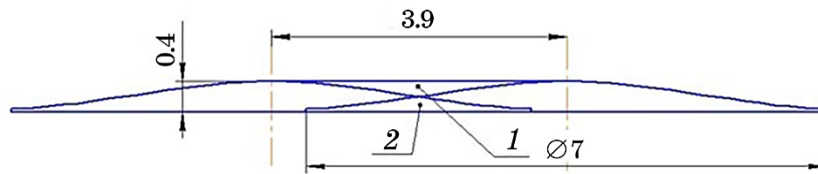**Fig. 9.** Adjacent runs of simulated sputtered solids for sample No. 1.

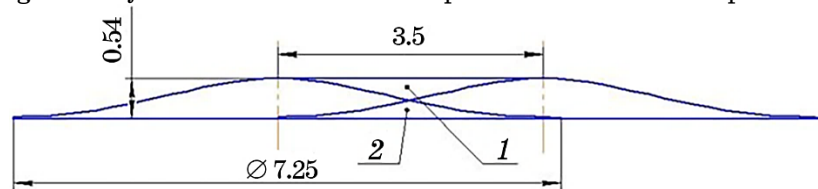**Fig. 10.** Adjacent runs of simulated sputtered solids for sample No. 2.

Fig. 11. Adjacent runs of simulated sputtered solids for sample No. 3.

in the sputtered solid height to 0.4 mm, the step of 56% will be optimal accounting for the diameter of the sputtered solid base. As the height increases to 0.54 mm, the optimal step between the run decreases, being 48% of the diameter of the sputtered solid base. Taking into account the obtained results, the technique for calculating the modes of the sputtering device movement relative to the component part being sputtered was proposed.

The technique for calculating the sputtering modes can better be explained on a particular example. Let us perform the calculation for a cylindrical surface, to which applied is the coating with the following dimensions: diameter $D = 39.6$ mm and length $L = 23$ mm. The calculation pattern is shown in Fig. 12 where: V_r is the component parts' rotation velocity during sputtering, V_g is the horizontal velocity of the sputtered solid movement (at point A) along the sputtering device, V is the sputtered solid velocity along the spiral trajectory of the sputtered solid movement, L is the length of the surface, which is processed, k is the step of the spiral trajectory. The diameter of the sputtered solid base is set within $d = 6$–12 mm, assuming $d = 6$ mm. It is necessary to sputter to the size of $D = 40.2$ mm.

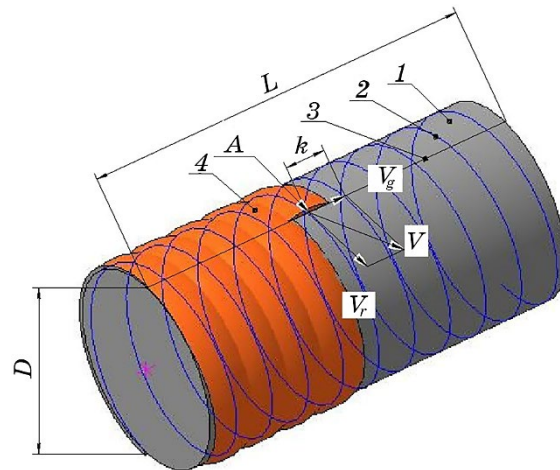Given that the work piece diameter after pre-machining is of 10 mm,

Fig. 12. Calculation pattern: component part to be sputtered (*1*), spiral trajectory of the sputtered-solid movement (*2*), a spiral trajectory of the sputtering-device movement along the component part (*3*), the coating being formed (*4*).

and the work piece diameter after sputtering, taking into account the allowance for mechanical processing, should be of 40 mm, the sputtering layer per side will be of 15 mm. To ensure the coating greater uniformity, it is advisable to divide this amount into 3 runs, each of which to be equal to 5 mm.

We determine the sputtered solid cross-sectional area S using known formulas or draw the coated solid designed profile, for example, using Kompas software and use the 'Mass-centring characteristics' function to determine the sputtered solid cross-sectional area, which is $S = 0.464$ mm^2. The length of the spiral one-turn b shall be determined using the Pythagorean theorem:

$$b = \sqrt{(\pi D)^2 + k^2} = \sqrt{(\pi \times 40)^2 + 5.24^2} = 125.71 \text{ mm}. \tag{13}$$

The number of turns shall be defined as follows:

$$n = \frac{L}{k} = \frac{27}{5.24} = 5.15. \tag{14}$$

The spiral total length shall be as follows:

$$B = nb = 125.71 \times 5.15 = 848.54 \text{ mm}. \tag{15}$$

Let us determine the sputtering-layer weight M. To do this, we multiply the cross-sectional area of sputtered solid S by the total length of spiral B and by the density of powder material ρ:

$$M = SB\rho = 0.464 \times 848.54 \times 0.0053 = 2.0867 \text{ g}. \tag{16}$$

The weight of total three-layer coating is as follows:

$$M_1 = M \times 3 = 2.0867 \times 3 = 6.26 \text{ g}. \tag{17}$$

The weight of total three-layer coating accounting for the coefficient of powder utilization, equalling for the gas-dynamic sputtering to 0.4 [2] for the entire surface coating, will require the sputtering powder

$$M_2 = \frac{M_1}{0.4} = \frac{6.26}{0.4} = 15.65 \text{ g}. \tag{18}$$

Let us determine the time of the three-layer coating sputtering:

$$t = \frac{M_2}{P} = \frac{15.65}{2} = 7.83 \text{ min}, \tag{19}$$

where $P = 2$ g/min is the sputtering device performance (device characteristics).

The time of one coating layer sputtering is

$$t_1 = \frac{t}{3} = \frac{7.83}{3} = 2.61 \text{ min}. \tag{20}$$

Let us calculate the sputtering device horizontal velocity V_g. To do this, we divide the horizontal movement path length L by the time of one coating layer sputtering, and determine the sputtering device horizontal movement velocity:

$$V_g = \frac{L}{t_1} = \frac{23}{2.61} = 8.81 \text{ mm/min}. \tag{21}$$

Let us determine the solid movement velocity along spiral trajectory:

$$V = \frac{B}{t_1} = \frac{848.54}{2.61} = 352.1 \text{ mm/min}. \tag{22}$$

Let us determine velocity V_l, at which the component part rotates:

$$V_l = \sqrt{V^2 - V_g^2} = \sqrt{352.1^2 - 8.81^2} = 351.99 \text{ mm/min}. \tag{23}$$

Let us determine the number of the component part revolutions per minute:

$$n = \frac{V_l}{b} = \frac{351.99}{125.71} = 2.8 \text{ rev/min}. \tag{24}$$

5. CONCLUSIONS

1. The design of the unit for cold-gas-dynamic sputtering of metal coatings, which allows adjusting the parameters of the gas-powder flow and, respectively, influencing the characteristics of the coating is developed.

2. The regularities of formation of cold-gas-dynamic sputtering solid profile in respect of aluminium-based powder coatings are studied.

3. The technique is proposed for calculating and simulating the profile of the sputtered solid depending on the sputtering device performance.

4. Using the information on the shape of the sputtered solid profile, the technique is developed for determination, depending on the sputtering device performance, of the device speed of movement along the component part, the speed of the component part rotation, the amount of powder required to cover the given surface and the sputtering time, with minimization of irrational loss of powder material having been ensured.

REFERENCES

1. A. I. Kashirin., O. F. Klyuev, and A. V. Shkodin, *Patent 2237746 Russian Federation*, MPK C 23 C 24/04, (2004) (in Russian).

2. A. P. Alhimov, S. V. Klinkov, V. F. Kosarev, and V. M. Fomin, *Kholodnoye Gazodinamicheskoye Napylenie. Teoriya i Praktika.* [Cold Gas-Dynamic Sputtering. Theory and Practice.] (Moskva: FIZMATLIT: 2010) (in Russian).

3. L. Yaroshenko, V. Bandura, L. Fialkovska, D, Kondratyuk, V. Palamarchuk, and Y. Paladiichuk. *Agraarteadus*, **32**, No. 2: 204 (2021).

4. O. Voznyak, A. Semenov, O. Semenova, A. Rudyk, B. Pinaiev, and R. Kulias, *Proceedings of the 2020 IEEE Ukrainian Microwave Week (UkrMW)*, (Kharkiv: 2020), vol. **2**, No. 2, p. 272.

5. O. L. Gaydamak, V. A. Matviychuk, and Yu. V. Kucherenko, *Engineering, Energy, Transport AIC*, **109**, No. 2: 105 (2020) (in Ukrainian).

6. V. Hraniak, V. Matviychuk, and I. Kupchuk, *Electronics,* **26**, No. 1: 69 (2022).

7. V. Matviychuk, O. Gaidamak, and M. Karpiychuk, *Vibration in Engineering and Technology*, **105**, No. 2: 65 (2022).

8. O. Gaidamak, *Engineering, Energy, Transport AIC*, **112**, No. 1: 46 (2021).

9. Yu. G. Vedmitskyi, V. V. Kukharchuk, V. F. Hraniak, I. V. Vishtak, P. Kacejko, and A. Abenov, *Proceedings of the SPIE*, No. 10808 (2018).

10. V. Matviychuk and M. Kolisnyk, *Vibration in Engineering and Technology*, **100**, No. 1: 111 (2021).

11. O. Gaidamak and V. Matviychuk, *Vibration in Engineering and Technology*, **102**, No. 3: 72 (2021).

12. V. A. Matviychuk, O. L. Gaydamak, and M. F. Karpiychuk, *Engineering, Energy, Transport AIC*, **116**, No. 1: 83 (2022) (in Ukrainian).

13. O. L. Gaidamak, *Patent 110552 Ukraine*, МПК C 23 C 24/00 (2014) (in Ukrainian).

14. A. Shtuts, M. Kolisnyk, A. Vydmysh, O. Voznyak, S. Baraban, and P. Kulakov, *Key Engineering Materials*, **844**: 168 (2020).